

# Imminent cardiac risk assessment *via* optical intravascular biochemical analysis

[††](#)David L. Wetzel <sup>\*a</sup>, Louis H. Wetzel <sup>b</sup>, Mark D. Wetzel <sup>c</sup> and Robert. A. Lodder <sup>d</sup><sup>a</sup>Microbeam Molecular Spectroscopy Lab., Kansas State University, Manhattan, KS, USA<sup>b</sup>Radiology Dept., University of Kansas Medical Center, Kansas City, KS, USA<sup>c</sup>Manhattan Medical Associates, Manhattan, KS, USA<sup>d</sup>Chemistry Dept., University of Kentucky, Lexington, KY, USA

Received 2nd December 2008, Accepted 23rd March 2009

First published on the web 9th April 2009

Heart disease is by far the biggest killer in the United States, and type II diabetes, which affects 8% of the U.S. population, is on the rise. In many cases, the acute coronary syndrome and/or sudden cardiac death occurs without warning. Atherosclerosis has known behavioral, genetic and dietary risk factors. However, our laboratory studies with animal models and human post-mortem tissue using FT-IR microspectroscopy reveal the chemical microstructure within arteries and in the arterial walls themselves. These include spectra obtained from the aortas of ApoE<sup>-/-</sup> knockout mice on sucrose and normal diets showing lipid deposition in the former case. Also pre-aneurysm chemical images of knockout mouse aorta walls, and spectra of plaque excised from a living human patient are shown for comparison. In keeping with the theme of the SPEC 2008 conference 'Spectroscopic Diagnosis of Disease...' this paper describes the background and potential value of a new catheter-based system to provide *in vivo* biochemical analysis of plaque in human coronary arteries. We report the following: (1) results of FT-IR microspectroscopy on animal models of vascular disease to illustrate the localized chemical distinctions between pathological and normal tissue, (2) current diagnostic techniques used for risk assessment of patients with potential unstable coronary syndromes, and (3) the advantages and limitations of each of these techniques illustrated with patent case histories, related in the first person, by the physician coauthors. Note that the physician comments clarify the contribution of each diagnostic technique to imminent cardiac risk assessment in a clinical setting, leading to the appreciation of what localized intravascular chemical analysis can contribute as an add-on diagnostic tool. The quality of medical imaging has improved dramatically since the turn of the century. Among clinical non-invasive diagnostic tools, laboratory tests of body fluids, EKG, and physical examination are still the first line of defense. However, with the fidelity of 64-slice CT imaging, this technique has recently become an option when the patient presents with symptoms of reduced arterial flow. Single photon emission computerized tomography (SPECT) treadmill exercise testing is a standard non-invasive test for decreased perfusion of heart muscle, but is time consuming and not suited for emergent evaluation. Once the invasive clinical option of catheterization is chosen, this provides the opportunity for intravascular ultrasound (IVUS) imaging. As the probe is pulled through the artery, the diameter at different parts is measurable, and monochrome contrast in the constricted area reveals the presence of tissue with a different ultrasonic response. Also, *via* an optical catheter with a fiber-optic conductor, the possibility of spectroscopic analysis of arterial walls is now a reality. In this case, the optical transducer is coupled to a near-infrared spectrometer. Revealing the arterial chemical health means that plaque vulnerability and imminent risk could be assessed by the physician. The classical emergency use of catheterization involves a contrast agent and dynamic X-ray imaging to locate the constriction, determine its severity, and possibly perform angioplasty, and stent placement.

## Introduction

Heart disease is by far the biggest killer in the Western world. In the United States, the 652 091 deaths attributed to heart disease in 2005 essentially equaled the number of deaths attributed to the next two causes, cancer and stroke, combined.<sup>1</sup> In coronary artery disease, the lumen through which the blood flows is either narrowed to the point that the flow is seriously reduced or blocked altogether (Fig. 1). In the latter case, sudden cardiac events including myocardial infarction and sudden cardiac death may occur. When the patient presents with an acute coronary syndrome, imminent risk assessment is essential. Post-mortem vibrational spectroscopy of arterial wall tissues has revealed chemical compositional preconditions related to risk. Atherosclerotic plaque contains variable amounts of calcium, lipids, proteins, and inflammatory cells depending upon the 'age' and 'vulnerability' of the plaque.

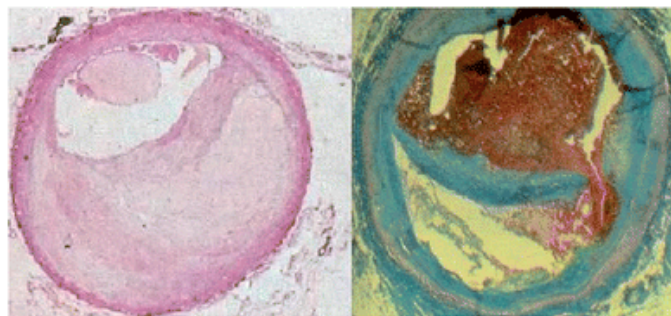


**Fig. 1** Human artery sections with lumen limited, due to plaque build up (left) and plaque rupture followed by severe thrombosis (right). Photomicrographs courtesy of Thomas Rosamond.

Prior to 2008, *in vivo* intravascular chemical analyses had not been available. Now that the U.S. Food and Drug Administration (FDA) has approved an optical catheter, a new add-on diagnostic tool is available to potentially enhance cardiac risk assessment in the near future. The present diagnostic procedures of angiography, intravascular ultrasound (IVUS), and X-ray computerized tomography (CT) are discussed in the context of patient history and care to provide the clinical perspective. The contribution of each technique to characterization of atherosclerotic plaque is considered. Also, the desirability of providing intravascular chemical information regarding the nature of the arterial wall and plaque deposition is illustrated. The chemical information that can be obtained *via* an intravascular catheter operating in the near-infrared region of the spectrum may be related to what has been previously observed with mid-infrared spectra obtained from FT-IR microspectroscopy of post-mortem tissue from ApoE<sup>-/-</sup> knockout mice and in one case plaque excised from a living human patient.

### Aorta wall vulnerability and atherosclerosis risk factors

Heart disease risk factors include (1) family history (genetic), (2) smoking, diet, lack of physical activity, and (3) diabetes, high cholesterol, and obesity. Only the behavioral risk factors can be reduced by the patient or by those of us in the general public. But if a patient is genetically predisposed to development of heart disease, medical vigilance is the prudent course. Many cardiovascular events such as sudden cardiac death occur without any warning. In the case of abdominal aortic aneurysm, the most vulnerable part of the aorta wall is the thin cap fibroatheroma. This vulnerability is due to the fact that the mechanical strength of the aorta wall is at a minimum at this locality compared with all other places.

### Experimental

All of the original experimental data reported in the first person by the authors of this paper were obtained from synchrotron infrared confocal microspectroscopy performed on beamline U10b of the vacuum ultraviolet storage ring at the national synchrotron light source (NSLS) of Brookhaven National Laboratory (BNL) Upton, New York. A Continuum™ infrared microscope (Spectra-Tech/Nicolet, Madison WI) interfaced to a Magna 650 FT-IR spectrometer (Nicolet/Thermo Fisher, Madison WI) was permanently installed on beamline U2b. The Continuum™ was equipped with a 50 μm dedicated, liquid nitrogen-cooled, mercury cadmium telluride detector that matched the infrared microbeam. Matching infinity corrected 32 times Schwartzchild mirror lenses were used as the objective and condenser. Confocal operation was achieved using a single image plane mask with a double pass before and after the microscope stage. To maximize signal for spectra collection the infrared focus was adjusted interactively while viewing the intensity of the single beam background spectrum.

A resolution of 8 cm<sup>-1</sup> was used and the microscope and spectrometer were purged continuously with boil-off nitrogen. For small image plane masking 256 scans were coadded and when masking approached the synchrotron beam size, 64 or 32 scans were coadded. In the transmission mode, microtomed frozen sections of tissue 4–6 μm thick were thaw-mounted onto BaF<sub>2</sub> (13 mm × 1 mm thick) windows and the background was collected from a part of the clean window. Compensation of the mirror lens was adjusted for transmission measurement to minimize spherical aberration introduced by the substrate. Infrared-reflecting (low *e*) glass slides were used to mount 4 μm thick tissue specimens in the reflection absorption operational mode and background spectra were obtained from a clear portion of the reflecting surface.

For purposes of imaging, the motorized stage was programmed to collect single spectra in a raster scan scheme and the resulting imaging raw data provided a full spectrum for each pixel. Organic functional group maps (images) were produced from baseline-corrected absorption band areas using Omnic™ software furnished with the microspectrometer. From each mapping experiment a family of images resulted, each highlighting the relative population of a particular chemical species at an individual *x,y* (pixel) location in the image.

## Results and discussion

### Animal model experimental results

In a previous FT-IR microspectroscopic study<sup>2</sup> we collected 80 000 mid-infrared spectra from a section of human brain tissue from the victim of massive hemorrhage from a brain aneurysm. Because the probe spot size was deliberately small ( $10\ \mu\text{m} \times 10\ \mu\text{m}$ ) and the target was large, we were unable to locate the specific weakened point within the thin cap; however, the chemical ratio gradient observed supported the concept of localized vulnerability.

The aorta sections of a male ApoE<sup>-/-</sup> knockout mouse that had been infused with angiotensin II (Ang II) enzyme from which typically 40% of the males develop aneurysms were extensively mapped in a raster scan pattern with synchrotron confocal microspectroscopy to produce various chemical images in a search for vulnerable segments in the aorta wall where the collagen I/elastin ratio was elevated. This particular mouse did not develop an aneurysm, however, from a highly spatially resolved map of a healthy wall segment with intima and adventitia of the aortic wall<sup>3</sup> being defined chemically<sup>4</sup> by the  $1740\ \text{cm}^{-1}$  carbonyl band indicative of lipid and the  $2927\ \text{cm}^{-1}$  CH stretching vibration from the hydrocarbon chain associated primarily with the lipids, as shown in Fig. 2. These experiments were pursuant to a study of aneurysm formation made possible by the previously known response of the male knockout mice to the enzyme. Fig. 3a and 3b show photomicrographs of two sections from the same aorta of an LDL<sup>-/-</sup> receptor deficient mouse on a C57BL/6 background obtained 50  $\mu\text{m}$  apart.<sup>5,6</sup> Shown left to right are the aorta with the wall intact and the ninth successive 5  $\mu\text{m}$  section having a break in the wall with an adjacent aneurysm. Fig. 3c shows a chemical image of the aorta wall and surrounding tissue. The  $1235\ \text{cm}^{-1}$  chemical image just inside the aorta wall protein shows potential vulnerability where elastin is less prevalent. The aneurysm image (Fig. 3d) shows heterogeneity with respect to the lipid at  $1469\ \text{cm}^{-1}$ .

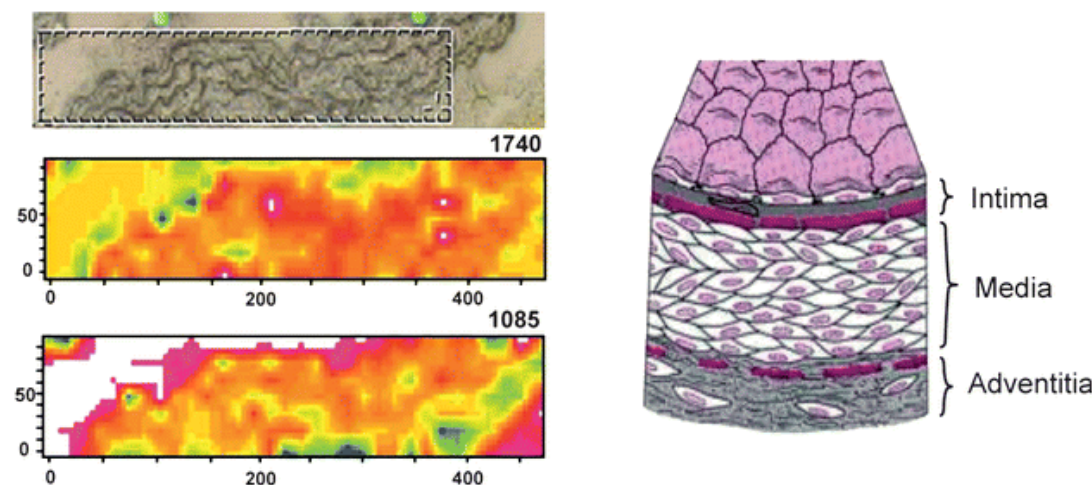


**Fig. 2** (Top left) Photomicrograph of unstained aorta wall. (Middle left) The image from  $1740\ \text{cm}^{-1}$  baseline-adjusted peak areas clearly defines the intima (inside of aorta wall). (Lower left) Image that chemically defines the adventitia (from ref. 4). (Right) Textbook drawing for clarification. (Reproduced with permission from ref. 3. Copyright 1979, W.B. Saunders.)

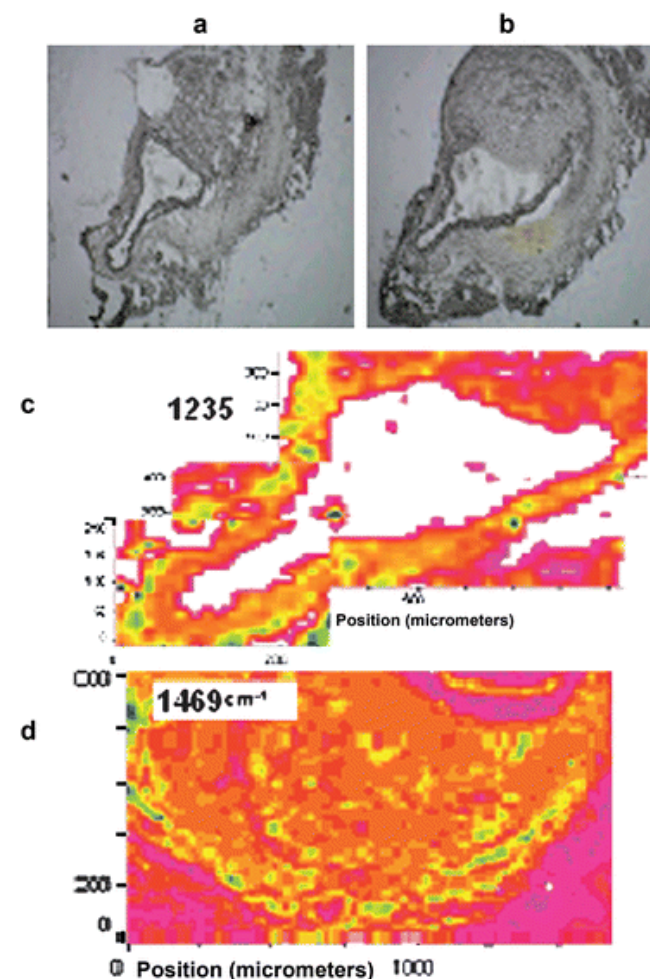


**Fig. 3** (a,b) Aneurysm progression along aorta segment. Aneurysm progression along knockout mouse aorta segments 50  $\mu\text{m}$  apart. Note intact aorta in section 1 (left) and ruptured in section 10 (right) with developed aneurysm. (c) (from part (a)) Image from  $1235\text{ cm}^{-1}$  baseline-adjusted peak area from several maps of the same aorta. At the position between 12 and 3 o'clock the aorta wall has been broken and aneurysm formation has taken place. Mapping of this tissue enables study of the localized chemical changes that just precede formation of an aneurysm. (d) Map of a large aneurysm observed at  $1469\text{ cm}^{-1}$ , representing lipid distribution (from [ref. 5](#). Reproduced with permission from [ref. 6](#). Copyright 2008, Wiley).

A paper by Urbas *et al.*<sup>7</sup> describes the use of near-infrared spectrometry of the ApoE<sup>-/-</sup> mouse to reveal collagen I/elastin ratios. Near-infrared spectra of ternary mixtures with known amounts of collagen I, collagen III, and elastin were used to develop an analytical expression. In these studies, infusion of the enzyme angiotensin II (Ang II) into the subcutaneous space of mice was done in doses ranging from 500 to 1000  $\text{ng kg}^{-1} \text{ min}^{-1}$  for 7–28 days. These were used as models of abdominal aortic aneurysm (AAA) development. This study showed that near-IR spectrometry and principal component regression (PCR) can be used to obtain the collagen/elastin ratio and determine the Ang II dose in a mouse aorta. A synchrotron infrared microspectroscopic experiment with ApoE<sup>-/-</sup> knockout mice aorta tissues was performed to look for enhanced collagen/elastin ratios in the mid-IR region of the spectrum in localized portions of the aorta wall.<sup>4</sup>

In regard to soft plaque characterization by high lipid  $1740\text{ cm}^{-1}$  band prominence, [Fig. 4a](#) and [4b](#) show the aortas of two mice.<sup>8</sup> [Fig. 4a](#) shows foam-like deposits lining most of the inside of the aorta of the mouse that was fed sucrose in its diet for 15 weeks. The aorta ([Fig. 4b](#)) of the control mouse fed a normal diet for the same period in contrast had only a single suspect area. The many spectra ([Fig. 4c](#) and [4d](#)) obtained from each of the foamy deposits inside of the walls all had varying but prominent  $1740\text{ cm}^{-1}$  carbonyl absorption bands. In contrast to the high lipid content of the plaque, the spectra of non-diseased arterial walls had prominent amide I and amide II bands at  $1650\text{ cm}^{-1}$  and  $1550\text{ cm}^{-1}$ , respectively. When this

area was probed, there was negligible absorption in the  $1740\text{ cm}^{-1}$  carbonyl region (Fig. 4e) and essentially no increased absorption in the  $2927\text{ cm}^{-1}$   $\text{CH}_2$  stretching region (not shown). Fig. 5 shows 3-D maps of the wall (outside) and the plaque (inside) for the  $1650\text{ cm}^{-1}$  and  $1740\text{ cm}^{-1}$  images, respectively. In contrast to the mouse, Fig. 6 shows spectra of plaque of a living human excised from the coronary artery during angioplasty in preparation for stenting; the highly prominent  $1740\text{ cm}^{-1}$  carbonyl bands are indicative of considerable lipid presence. Unlike calcified plaque or fibrous plaque, a greater imminent risk is that presented by soft plaque that has predominantly lipid characteristics. Unstable plaque may rupture suddenly, exposing the intima of the vessel and resulting in a cascade of events including platelet aggregation, thrombus formation, and coronary occlusion leading to clinical events such as myocardial infarction and/or sudden cardiac death.

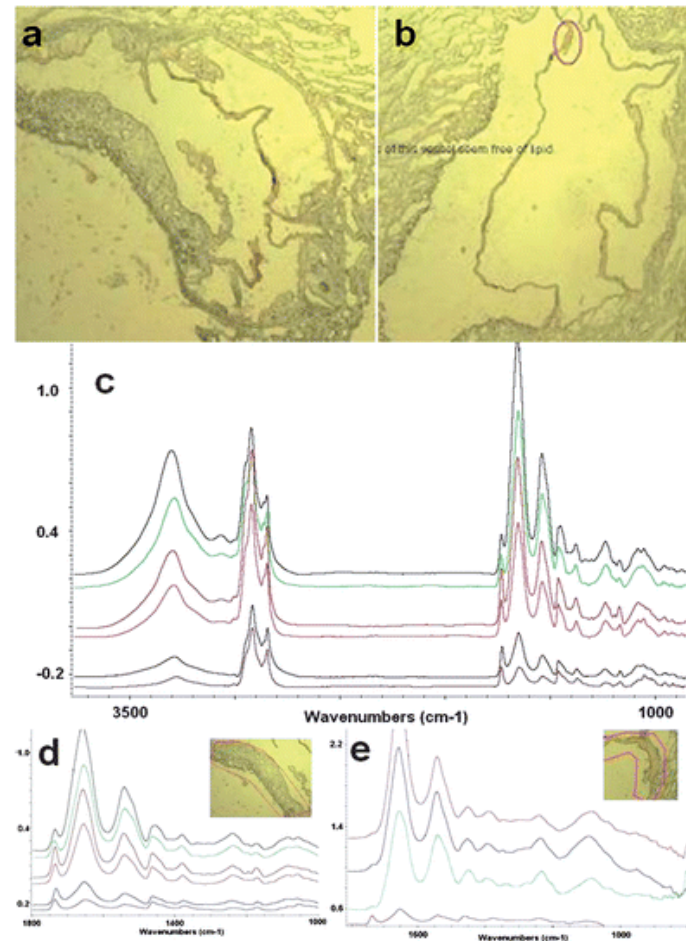


**Fig. 4** (a,b) Photomicrographs of aorta frozen section of mole knockout mouse (left) on carbohydrate diet showing foamy deposits lining the walls. Note contrast with aorta wall (right) of mouse on normal diet. (c,d) Full spectra and an enlarged fingerprint region of foaming deposit shown in (a). In the aorta spectra at high lipid locations in the sucrose fed mouse, note CH bands at  $2927\text{ cm}^{-1}$  and  $1469\text{ cm}^{-1}$ ; also carbonyl bond at  $1740\text{ cm}^{-1}$ . Protein in the aorta wall produces prominent amide I and amide II bands at  $1650\text{ cm}^{-1}$  and  $1550\text{ cm}^{-1}$  respectively. (e) Aorta spectra from control mouse.

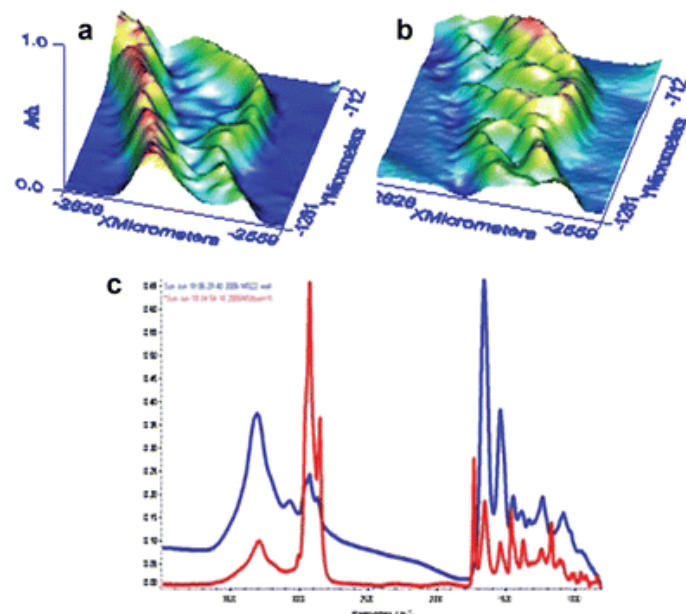


**Fig. 5** (a) Image highlighting the protein of an aorta cell wall. (b) Image highlighting the lipid of spongy material adhering to the aorta wall. (c) Spectra (blue) wall and (red) spongy material are from corresponding highlighted parts, respectively. The tissue was from an ApoE<sup>-/-</sup> knockout mouse that was fed a sucrose diet.

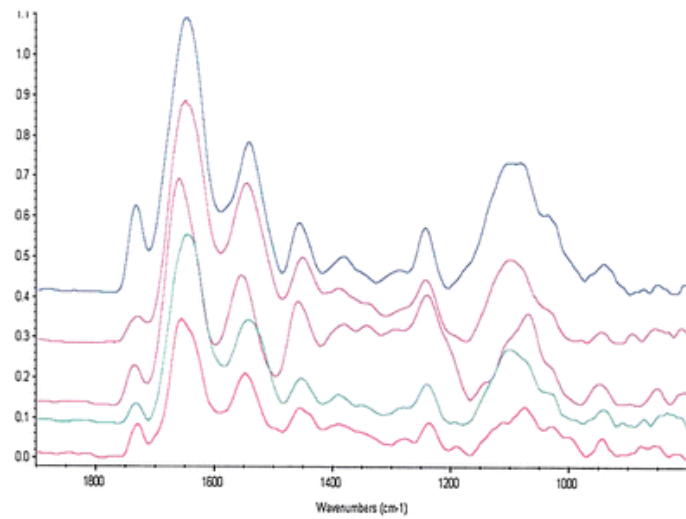


**Fig. 6** Spectra of lipid-containing plaque from human artery showing prominent 1740 cm<sup>-1</sup> carbonyl bands.

**Conventional cardiac imaging**

The thallium treadmill test is among the non-invasive techniques used in evaluation of ischemic cardiac disease. A positive treadmill test usually leads to an invasive technique such as angiography (catherization) sometimes accompanied by intravascular ultrasound (IVUS) imaging. With the recent drastically improved fidelity (Fig. 7) of the 64-slice X-ray computerized tomography (CT), this radiological technique in the cardiology diagnostic setting is emerging as another valuable non-invasive imaging technique. The relative advantages of these cardiac imaging tools are illustrated in Fig. 8. Angiography provides information only about the lumen (the passage through which the blood flows) but little information about the arterial walls or plaque. CT provides information about the lumen and surrounding arterial wall, but can only characterize the plaque as calcified or non-calcified. It is currently limited in its ability to distinguish stable fibrotic soft plaque from lipid-laden unstable soft plaque. On the other hand, IVUS provides the most reliable quantitative information

regarding narrowing of the lumen and has some ability to characterize soft plaque with the ultrasound image. Although a positive treadmill test triggers further testing and possible interventional procedures such as angioplasty, a negative treadmill test does not necessarily indicate future well-being of the patient. Author D. L. W. experienced a cardiac event within only a few months after having passed a treadmill test. Case III, presented later in this paper, involved a similar circumstance with fatal outcome. In the clinical cases that follow, an argument can be made for the desirability of intravascular chemical characterization as an add-on technique to enhance existing conventional catheterization techniques.

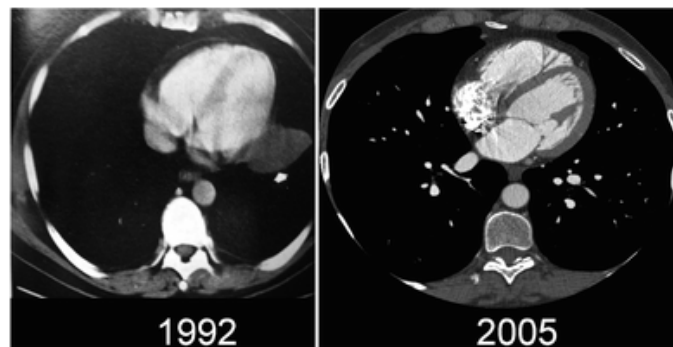


**Fig. 7** Comparison of image clarity between one-slice CT (left) and 64-slice CT (right) with smaller pixel size and faster helical scanning.

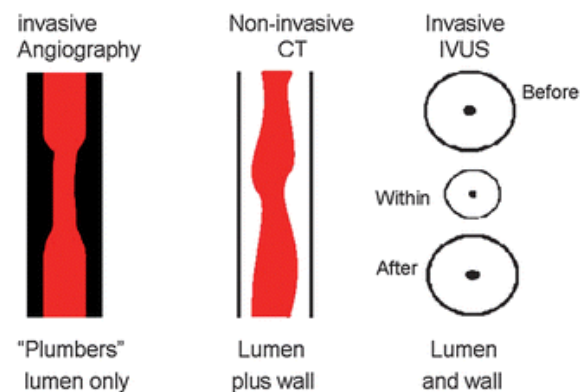


**Fig. 8** Imaging technique diagrams (left to right) of invasive angiography, non-invasive CT and invasive IVUS. Angiography only shows an outline of the vessel lumen and gives no information about the vessel wall. CT shows the lumen and gives limited information about plaque within the wall of the vessel. IVUS depicts the lumen and gives some characterization of plaque within the vessel wall.

### Case I

A 52-year-old woman presented with acute cardiac symptoms in the emergency room of a suburban hospital where she received 16-slice CT chest imaging and other routine diagnostic tests which were negative for myocardial infarction. She spent the night in the hospital and was released and sent home. At work on the following Monday, she again experienced symptoms, and on Tuesday in the ER of a teaching/research hospital at the request of the attending cardiologist, a 64-slice coronary CTA was administered. From the CT slice just below the aortic arch (Fig. 9a and 9b), the constriction problem of the left anterior descending artery was revealed. The 3-D image in Fig. 9c and 9d clearly shows the narrowing of this important artery. The invasive technique of angiography (Fig. 10a) provided the outline of the lumen as predicted from the CT in Fig. 10b. Intravascular ultrasound on the same patient (Fig. 11) shows a succession of still images taken from the active video showing the full normal internal dimension beyond the plaque, progressive narrowing of the lumen, maximum narrowing at the middle of the plaque, decreasing narrowing, and finally full normal dimension above the plaque.<sup>9</sup> Closer examination of the area of major constriction shows a dark region in the sonographic image (Fig. 12) suggesting unstable plaque. Chemical analysis of this dark region would have added value to the diagnosis by confirming high lipid concentration in the plaque. Chemical analysis would add to the cardiologist's confidence in the diagnosis of unstable plaque and provided

additional evidence of the need for angioplasty and stenting in addition to aggressive medical therapy. For this patient, angioplasty stenting was performed resulting in the patent artery shown in [Fig. 13](#), and she remains free of symptoms two years later. In this case, the enhanced resolution power of the 64-slice CT led to rapid diagnosis and treatment.

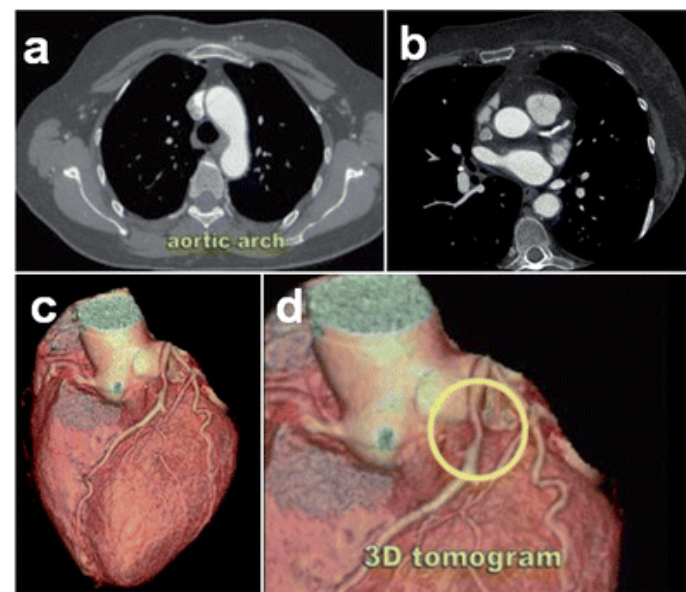


**Fig. 9** (a,b) 64-slice cardiac CT transverse slices at aortic arch and level where narrowed artery was found. (c,d) Colorized 3-D reformations of CT data showing whole heart and zoom of narrowed arterial segment.



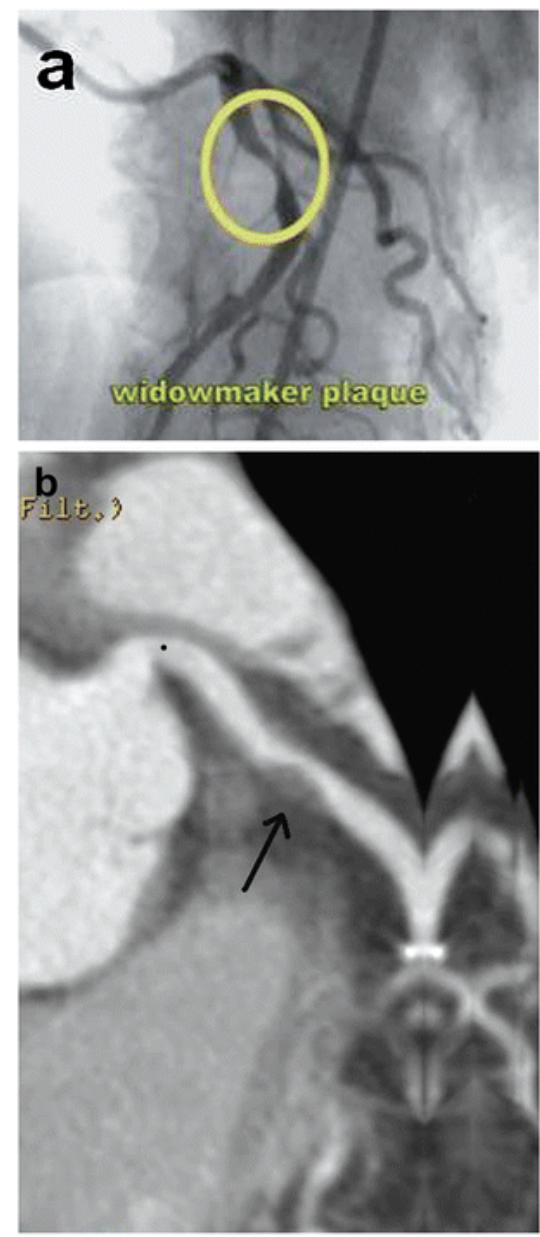


**Fig. 10** (a) Angiogram (X-ray with contrast agent) done after CT scan shows markedly narrowed left anterior descending artery. (b) CT vertical reformation shows large soft plaque (arrow) narrowing the lumen of the artery profile with narrow segment.

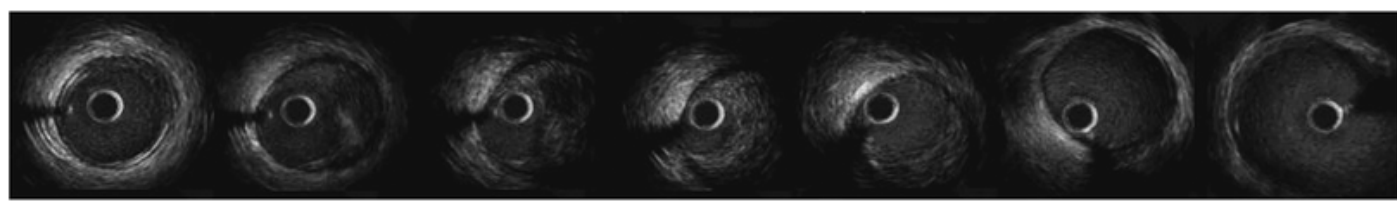


**Fig. 11** Series of IVUS frames going from normal diameter below plaque (at left) to minimum diameter within plaque (center image) to normal diameter above plaque. Black dot is the ultrasound probe catheter within the vessel. IVUS showed 87% decrease in cross-sectional area of the vessel lumen.

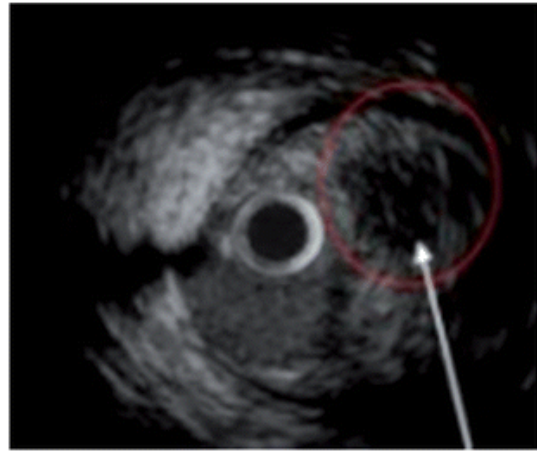


**Fig. 12** IVUS image within plaque shows dark region suggesting unstable plaque with high lipid content.



**Fig. 13** Post-angioplasty angiographic image of opened left anterior descending artery. Compare with stenosis in [Fig. 10a](#).

### Case II

A 69-year-old professor presented with shortness of breath and chest tightness with minimal exertion. He underwent angiography, revealing severe 3-vessel coronary artery disease, and bypass surgery was planned for the following week. His symptoms worsened, and he was felt to have a highly unstable area of recent thrombosis involving the proximal left anterior descending artery, thus the patient was taken to urgent bypass surgery. This case is illustrative in that optical catheter biochemical characterization of this area would have demonstrated high levels of the proteins fibrin and thrombin, citing the lesion as highly unstable with need for immediate revascularization.

### Case III

In 2008, a 58-year-old journalist died suddenly while at work. His physician indicated that a cholesterol plaque ruptured causing coronary thrombosis and sudden cardiac death. He had been under the care of a cardiologist and diagnosed with asymptomatic coronary artery disease that had been apparently well controlled with medication and exercise. He had performed well on a stress test within six months prior to his death. This case is illustrative of the all too common occurrence of sudden cardiac death of individuals in the prime of their lives. This also underscores the need for development of better methods for identification of high-risk patients than are currently in widespread use.

### Summary and potential for the future

Multidetector cardiac CT is a new technique which allows non-invasive detection of significant coronary artery plaque. Once

invasive catheterization is chosen for further evaluation of significant lesions or for acutely symptomatic patients, then chemical characterization *via* intravascular spectroscopy could also be performed to provide reliable additional information regarding the nature and vulnerability of the plaque. This should help guide immediate patient care decisions, and may help predict the risk of future morbidity and mortality. Based on the spectroscopic evaluation of plaque it is possible that a risk parameter could be developed (relative vulnerability index – RVI). This is exciting because it may allow physicians to use aggressive preventive medical therapy more effectively in the subset of patients that undergo angiography. With the optical catheter,<sup>10</sup> which after 8 years of review by the U.S. FDA is now available along with the spectrometer and dedicated software, the potential for such clinical use is within reach.

### Near-infrared catheter system and use

In this instrument, radiation from a tunable laser is propagated through a single fiber to the arterial wall that is being investigated. Radiation not absorbed by the plaque or the arterial wall is collected and transmitted to the near-infrared spectrometer *via* a second fiber. The resulting spectrum is produced in a time sequence.

Processing the data with custom multivariate statistical software enables the user of the optical catheter to receive a direct chemical assessment in objective terms. The near-infrared region of the spectrum is used because it penetrates the tissue that the probe encounters rather than analyzing only the surface and because the near-infrared radiation can be readily transmitted by fiber-optics.

[Fig. 14a](#) shows the spectrum of human plaque. For comparison, a spectrum of crystalline cholesterol is shown in [Fig. 14b](#). The near-infrared bands shown in the first figure are derived from the mid-infrared bands previously seen both in the human plaque mid-infrared spectrum and in the mid-infrared spectrum of the mouse aorta foamy area. Combination bands of the C–H stretch at 2927  $\text{cm}^{-1}$  and either the carbonyl band at 1740  $\text{cm}^{-1}$  or the C–H bend at 1469  $\text{cm}^{-1}$  are possibly the origin of the bands in the near-infrared shown at 5000  $\text{cm}^{-1}$  or 2300 nm. At the 7000  $\text{cm}^{-1}$  (1700 nm) are the overtones of bands found in the mid-infrared. Unlike the mid-infrared bands, the near-infrared requires interpretative software to get the full benefit from the raw data. The commercial near-infrared clinical system is equipped with custom software for preprocessing the data and translating it into medically interpretable statements.

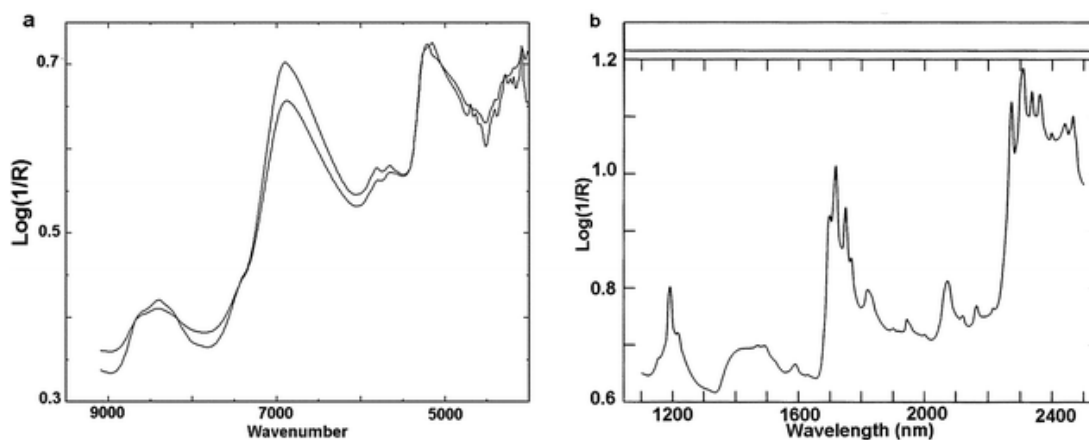


**Fig. 14** Near-infrared spectrum of (a) human plaque and (b) crystalline cholesterol. Note prominent bands at 2300 nm and 1700 nm due to CH combination bands and CH overtone bands, respectively corresponding to (a) 5800  $\text{cm}^{-1}$  and (b) 6800  $\text{cm}^{-1}$ .

### Case IV

In 2008, the first patient in the United States to be diagnosed with the newly available near-infrared catheter was a 70-year-old man in Royal Oak, Michigan. In this case, the diagnostic benefit that resulted was that the length of the plaque revealed from the lipid deposition was found to be greater than the length estimated from the physical morphological image ([Fig. 15](#)). Since pre-stent and post-stent restenosis (narrowing) are common causes of stent failure, choosing the right length stent based on chemical analysis may help reduce the rate of this occurrence.

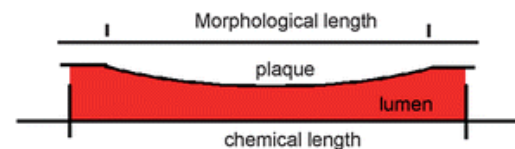


**Fig. 15** Diagram to illustrate dimensional difference in plaque measurements between the morphological length from CT or angiography and the chemical (lipid) length obtained with the intravascular near-infrared spectroscopic chemical diagnostic probe.

The presence of diabetes mellitus has very significant predictive value for coronary artery disease. In fact, the most recent American Heart Association guidelines recommend treating all type II diabetes patients as if they already have coronary artery disease. Glucose and insulin metabolism clearly play a key role in atherosclerosis and plaque formation. One glance at the mouse aorta lined with lipid-containing foamy depositions and the spectra taken from these depositions is a convincing argument for the risk factor that diabetes imposes on the arteries.

It should be emphasized that the enthusiasm expressed for intravascular chemical analysis of arterial walls must be tempered by the fact that this is a potential add-on technique. The actual value contributed is yet to be determined by the cardiologists working along with the radiologists performing this newly suggested test as well as the conventional tests. We must be reminded that the most dangerous threat is from the soft plaque, which is often undetected by conventional radiological imaging. The sudden rupture of this plaque may cause unstable coronary syndromes and death. In the management of patients it is essential to make every effort to detect latent threats such as this. In fact, there is good evidence that the majority of fatal coronary artery events are the result of rupture of unstable moderate-size plaques rather than high-grade stenotic plaques. This underscores the importance of not just detecting the degree of stenosis, but rather the true chemical nature of the plaque. The frequently reported 'calcium score' for coronary arteries is merely a record of the cumulative mineralization of plaque in a particular patient. It gives no indication as to the degree of arterial narrowing or the presence or nature of soft plaque. The mineralized plaque, or fibrous plaque, may very well have stability. Unstable plaque is vulnerable plaque. For example, consider Fig. 12 of the intravascular ultrasound, where the IVUS image showed an area of unknown deposition. Knowing whether this is a lipid or fibrous could make a difference in how aggressively the cardiologist treats such a case. The cardiology community has recently come under attack for overuse of angioplasty and stenting.<sup>11</sup> This is because they tend to treat any questionable plaque since their decision is based on morphologic criteria, *i.e.* what it looks like. It is likely that increased use of chemical analysis of plaque may show that many plaques do not have significant lipid content and therefore are fibrous and stable. Such patients may do well on medical therapy alone, and the cost and risk of stenting may possibly be avoided.

Chemical diagnosis of plaque is now a reality. At the present time, the intravascular near-infrared catheter and spectrometer is in use at at least six clinical facilities in the United States. In theory this device offers great promise to improve the treatment of coronary atherosclerosis. When and how it is best used, and whether its use has long term benefit, are yet to be determined.

## Acknowledgements

Synchrotron infrared microspectroscopy was performed at beamline U10b of the National Synchrotron Light Source of Brookhaven National Laboratory, Upton, NY, a user facility of the Department of energy under contract no. BEACO298CH10886. The technical assistance of Tiffany Fisher and Hicran Koc in data processing of animal model experiments and Lauren Brewer in assembly of graphics and manuscript preparation is sincerely appreciated.

## References

- 1 US Dept of Health 2005 and Human Services, *Leading Causes of Death*, National Center for Health Statistician review, April 11, 2008, <http://www.cdc.gov/nchs/fastats/lcod.htm>.
- 2 D. L. Wetzel, G. R. Post and R. A. Lodder, Synchrotron infrared microspectroscopic analysis of collagens I, III, and elastin on the shoulders of human thin-cap fibroatheromas, *Vib. Spectrosc.*, 2005, **38**, 53–59 [[Links](#)].
- 3 R. Ross, The pathogenesis of atherosclerosis, in *Heart Disease: A Textbook of Cardiovascular Medicine*, ed. E. E. Braunwald, W.B. Saunders, Philadelphia, 5th edn, 1979, pp. 1105–1125.
- 4 D. L. Wetzel, L. A. Cassis, M. Helton, R. A. Lodder. 2009. Synchrotron infrared microspectroscopy of potentially abnormal aorta tissue from enzyme infused male ApoE<sup>-/-</sup> knockout mouse, in preparation.
- 5 D. L. Wetzel and R. A. Lodder, Infrared microspectroscopic imaging of aorta sections of LDL<sup>-/-</sup> receptor deficient mice, 2008, in preparation.

- 6 D. L. Wetzel, Biomedical Applications of Infrared Microspectroscopy and Imaging by Various Means, in *Biomedical Vibrational Spectroscopy*, eds. P. Lasch and J. Kniepp, Wiley, New York, 2008, ch. 3, pp. 39–77.
  - 7 A. Urbas, M. W. Manning, A. Daugherty, L. A. Cassis and R. A. Lodder, Near-infrared spectroscopy of abdominal aortic aneurysm in the ApoE<sup>-/-</sup> mouse, *Anal. Chem.*, 2003, **75**(14), 3650–3655 [[Links](#)].
  - 8 R. A. Lodder and D. L. Wetzel, Synchrotron infrared microspectroscopic diet studies of ApoE<sup>-/-</sup> knockout mice aortas, 2009, in preparation.
  - 9 D. L. Wetzel, L. H. Wetzel, M. D. Wetzel and R. A. Lodder, at *Spec 2008 Shedding Light on Disease: Optical Diagnosis of Disease for the New Millennium*, held at São José dos Campos, Brazil, October 2008, oral presentation no. 3, Proceedings, eds. A. Martin and D. Zezel, pp. 5–8.
  - 10 P. Moreno, R. A. Lodder, W. O'Connor and J. E. Muller, *Method and apparatus for in vivo identification and characterization of vulnerable atherosclerotic plaques*, *US Pat.*, # 6,816,743, Nov. 9, 2004.
  - 11 W. E. Boden, R. A. O'Rourke, K. K. Teo, P. M. Hartigan, D. J. Maron, W. J. Kostuk, M. Knudtson, M. Dada, P. Casperson, C. L. Harris, B. R. Chaitman, L. Shaw, G. Gosselin, S. Nawaz, L. M. Title, G. Gau, A. S. Blaustein, D. C. Booth, E. R. Bates, J. A. Spertus, D. S. Berman, G. B. J. Mancini and W. S. Weintraub, Optimal Medical Therapy with or without PCI for Stable Coronary Disease, *New Engl. J. Med.*, 2007, **356**(15), 1503–1516 [[Links](#)].
- 

## Footnotes

† This paper is part of an *Analyst* themed issue on Optical Diagnosis. The issue includes work which was presented at SPEC 2008 Shedding Light on Disease: Optical Diagnosis for the New Millennium, which was held in São José dos Campos, São Paulo, Brazil, October 25–29, 2008.

‡ Contribution no. 09-158J, Kansas Agricultural Experiment Station, Manhattan, KS, USA.

---

**This journal is © The Royal Society of Chemistry 2009**